Progress In Electromagnetics Research, PIER 81, 253–265, 2008

FDTD STUDY ON WAVE PROPAGATION IN LAYERED STRUCTURES WITH BIAXIAL ANISOTROPIC METAMATERIALS

M. Y. Wang and J. Xu

School of Physical Electronics
University of Electronic Science and Technology of China
Chengdu, Sichuan 610054, China

J. Wu

National Key Laboratory of Electromagnetic Environment
China Research Institute of Radiowave Propagation
Beijing 102206, China

B. Wei, H. L. Li, T. Xu, and D. B. Ge

Physics Department
Xidian University
Xi'an, Shanxi 710071, China

Abstract—The Gaussian beam propagation in multi-layered structures that include indefinite anisotropic metamaterial (AMM) are simulated with shift operator method in Finite-Difference Time-Domain method (FDTD). The excitations of backward and forward surface affected by the types of biaxial AMM are investigated. Numerical results show that the directions of the guided wave excited are influenced by the sign of z component of relative permeability tensor of AMM that determines the energy flow is positively refracted or negatively refracted. Positive or negative Goos-Hänchen shift associated with Total Cutoff media are also shown.

1. INTRODUCTION

A medium with negative permittivity and permeability was introduced by Veselago in 1968 [1]. In 2001, inspired by the work of Pendry et al. [2] and Shelby et al. [3] foremost constructed a composite "medium" in the microwave regime by arranging periodic arrays of

small metallic wires and split-ring resonators (SRRs). These kinds of media can also be mentioned as metamaterials, negative-index materials, and left-handed medium [4, 5] etc. Soon, Alternative realizations of metamaterials that consisted of host transmission lines with embedded lumped series capacitors and shunt inductors are proposed and realized [6].

The structures (interlacing wires and split-ring resonators) investigated in experiments are strongly anisotropic [7, 8]. Lindell et al. [9] firstly exposed the study of waves in anisotropic metamaterial (AMM), which does not necessarily require all tensor elements of $\boldsymbol{\varepsilon}$ and $\boldsymbol{\mu}$ have negative values. The concepts of refraction of wave vector and Poynting power in indefinite AMMs have been exposed in [10]. Some propagation characteristics of electromagnetic (EM) waves associated with AMM have been analytically discussed. Such as negative Goos-Hänchen shift [11, 12], anomalous reflection, total reflection [13], and total transmission [14] at the interfaces between isotropic regular media and AMM et al. Anisotropic metamaterials have potential applications in polarizing beam splitter [15], a band separating device [16], solid-state spectroscopy, and Omnidirectional linear polarizer et al.

Finite-Difference Time-Domain (FDTD) method is a popularly numerical algorithm to predict the properties of metamaterial that are made of SRRs and metallic wires [17] and are equivalent to dispersive media [18–25]. For the latter case, Lossy Drude polarization and magnetization models are often used to simulate the metamaterial with auxiliary differential equation (ADE) method in FDTD. The shift operator method is simple and avoids the introduction of electromagnetic currents or z-transform. The problem which incorporates both anisotropy and frequency dispersion at the same time can be solved for the AMM slabs.

The paper is organized as follows. We first present the biaxial anisotropic metamaterials and the schematic geometry of multi-layered structures that include an AMM for the excitation of surface waves and guided waves in Section 2. Section 3 derives the shift operator method in FDTD for the constitute relation of metamaterials. In Section 4, the interaction between Gaussian beam and multi-layered structures that include indefinite anisotropic metamaterial are simulated with FDTD to study its application in solid-state spectroscopy and linear polarizer et al. Meanwhile the wave vector and energy flow density in AMM are analyzed. Finally, conclusions are given.

2. BIAXIAL AMM AND EXCITATION OF GUIDED WAVES

2.1. The Classification of Four Types of Biaxial Anisotropic Metamaterials

The relative permittivity and permeability tensors of anisotropic metamaterial can be diagonalized as

$$\boldsymbol{\varepsilon} = \begin{bmatrix} \varepsilon_x & 0 & 0 \\ 0 & \varepsilon_y & 0 \\ 0 & 0 & \varepsilon_z \end{bmatrix} \quad \boldsymbol{\mu} = \begin{bmatrix} \mu_x & 0 & 0 \\ 0 & \mu_y & 0 \\ 0 & 0 & \mu_z \end{bmatrix} \tag{1}$$

where ε_i and μ_i $(i = x, y, z)$ are the relative permittivity and permeability constants in the principal coordinate system.

For the sake of brevity, only the TE-polarized wave case is discussed in the paper. The dispersive relation of wave in AMM for the TE-polarized waves can be written as

$$\frac{q_x^2}{\varepsilon_y \mu_z} + \frac{q_z^2}{\varepsilon_y \mu_x} = \frac{\omega^2}{c^2} \tag{2}$$

where q_i represent the i component of wave vector in AMM. From Eq. (2), one can find that the dispersive curves for AMM can be ellipse or hyperbola depending on the signs of $\varepsilon_y \mu_z$ and $\varepsilon_y \mu_x$.

As shown in reference [10], indefinite AMMs are identified as four classes of media based on their cutoff properties of wave vector q_x. Each type of the AMMs has two subtypes. Table 1 gives the classification of the four types of AMMs.

Table 1. The classification of four types of anisotropic metamaterials.

Type	Cutoff		Never Cutoff		Anti-Cutoff		Always Cutoff	
Subtype	I	II	I	II	I	II	I	II
Media condition	$\varepsilon_y<0$ $\mu_x<0$ $\mu_z<0$	$\varepsilon_y>0$ $\mu_x>0$ $\mu_z>0$	$\varepsilon_y<0$ $\mu_x<0$ $\mu_z>0$	$\varepsilon_y>0$ $\mu_x>0$ $\mu_z<0$	$\varepsilon_y>0$ $\mu_x<0$ $\mu_z>0$	$\varepsilon_y<0$ $\mu_x>0$ $\mu_z<0$	$\varepsilon_y<0$ $\mu_x>0$ $\mu_z>0$	$\varepsilon_y>0$ $\mu_x<0$ $\mu_z<0$
Propagation	$\theta < \theta_c$		Any θ		$\theta > \theta_c$		No real q_x	

In Table 1, θ is incident angle and θ_c is critical angle separating propagating from evanescent solutions. The propagation conditions are also given in Table 1. Total reflection occurs for Always Cutoff media at any angle and for Cutoff media if incident angle $\theta > \theta_c$ or for Anti-Cutoff media if $\theta < \theta_c$.

2.2. Excitation of Guided Waves

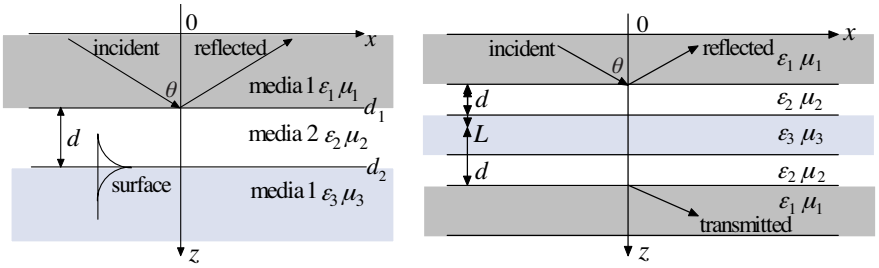

(a) The excitation of surface waves (b) Geometry of five-layered stucture

Figure 1. Schematic geometry of multi-layered structures that include biaxial anisotropic metamaterials.

Figure 1(a) schematically depicts a two-dimensional, three-layered structure. The time harmonic factor of the monochromatic plane wave is $\exp(\mathrm{i}\omega t)$. The input wave comes from an optically dense medium with $\varepsilon_1\mu_1 > \varepsilon_2\mu_2$ at an incident angle θ larger than the angle of total internal reflection. Medium 2 represents a gap layer of width d that separates medium 1 and 3. The third medium is assumed to be an AMM. Surface waves can be excited resonantly and supported by the interface between medium two and three under some conditions. Fig. 1(b) shows the five-layered structure geometry. There are two air gaps with material parameters ε_2 and μ_2. Without the first and fifth optically dense medium slabs with ε_1 and μ_1, the structure reduces to an anisotropic metamaterial isolated slab, which can support guided modes.

The reflection and transmission coefficients for the scattering of monochromatic plane waves by the multi-layered structures shown in Fig. 1 can be derived using the boundary conditions and transfer-matrix method. The lateral shift of the reflected and transmitted Gaussian beam affected by the angle of incidence, gap width, beam width and anisotropic metamaterial parameters et al. can be analytically discussed with the formula in reference [11] based on the reflection and transmission coefficients.

3. SHIFT OPERATOR METHOD IN 2D-FDTD SIMULATOR

The Maxwell equations are

$$\nabla \times \boldsymbol{E} = -\partial \boldsymbol{B}/\partial t \quad \nabla \times \boldsymbol{H} = \partial \boldsymbol{D}/\partial t \tag{3}$$

In the frequency domain, the constitute relation of anisotropic metamaterial can be described as

$$\boldsymbol{D} = \varepsilon_0 \boldsymbol{\varepsilon}(\omega)\boldsymbol{E} \quad \boldsymbol{B} = \mu_0 \boldsymbol{\mu}(\omega)\boldsymbol{H} \tag{4}$$

For TE wave case, B_x in Eq. (3) is discretized by using Yee's scheme

$$B_x^{n+1/2}\left(i,\, k+\frac{1}{2}\right) = B_x^{n-1/2}\left(i,\, k+\frac{1}{2}\right) + \Delta t \frac{E_y^n(i,\, k+1) - E_y^n(i,\, k)}{\Delta z} \tag{5}$$

Lossy Drude polarization and magnetization models [18–20] are often used to simulate the isotropic metamaterial. In the frequency domain, this means the relative permittivity and permeability are described as

$$\begin{aligned} &\varepsilon(\omega) = 1 - \omega_{pe}^2/[\omega(\omega + \mathrm{j}\Gamma_e)] \\ &\mu(\omega) = 1 - \omega_{pm}^2/\left[\omega(\omega + \mathrm{j}\Gamma_m)\right] = \sum_{n=0}^{N} p_n(\mathrm{j}\omega)^n / \sum_{n=0}^{N} q_n(\mathrm{j}\omega)^n \end{aligned} \tag{6}$$

where ω represents incident wave frequency, ε_0 and μ_0 differently represent vacuum permittivity and permeability. ω_{pe}, ω_{pm}, Γ_e and Γ_m represent electric plasma frequency, magnetic plasma frequency, electric plasma damping frequency and magnetic plasma damping frequency respectively. In Eq. (6), $n = 2$, and

$$\begin{aligned} &p_0 = \omega_{pm}^2, \quad p_1 = \Gamma_m, \quad p_2 = 1 \\ &q_0 = 0, \qquad q_1 = \Gamma_m, \quad q_2 = 1 \end{aligned} \tag{7}$$

The discretized H_x in the 2D-FDTD simulators are

$$H_x^{n+\frac{1}{2}} = \left[\left(a_0 B_x^{n+\frac{1}{2}} + a_1 B_x^{n-\frac{1}{2}} + a_2 B_x^{n-\frac{3}{2}}\right)/\mu_0 - b_1 H_x^{n-\frac{1}{2}} - b_2 H_x^{n-\frac{3}{2}}\right]/b_0 \tag{8}$$

which is an iterative formulation to calculate $H_x^{n+1/2}$, where

$$\begin{aligned} &a_0 = q_0 + 2q_1/\Delta t + q_2(2/\Delta t)^2 \quad &&b_0 = p_0 + 2p_1/\Delta t + p_2(2/\Delta t)^2 \\ &a_1 = 2q_0 - 2q_2(2/\Delta t)^2 \quad &&b_1 = 2p_0 - 2p_2(2/\Delta t)^2 \\ &a_2 = q_0 - 2q_1/\Delta t + q_2(2/\Delta t)^2 \quad &&b_2 = p_0 - 2p_1/\Delta t + p_2(2/\Delta t)^2 \end{aligned} \tag{9}$$

To compute $H_x^{n+1/2}$ with the peak power $N = 2$ of the complex relative permeability, w.r.t. $\mathrm{j}\omega$ in Padé approximation, $B_x^{n-3/2}$, $H_x^{n-3/2}$, $B_x^{n-1/2}$, $H_x^{n-1/2}$ and $B_x^{n+1/2}$ should have been computed. The formulation of $\boldsymbol{D}$ and $\boldsymbol{E}$ are the same as $\boldsymbol{B}$ and $\boldsymbol{H}$.

To sum up, the processes about the shift operator method in FDTD for AMM can be summarized

(i) The components of $\boldsymbol{B}^{n+1/2}$ are computed from $\boldsymbol{E}$ like Eq. (5).
(ii) The components of $\boldsymbol{H}^{n+1/2}$ are obtained from $\boldsymbol{B}$ just as Eq. (8).
(iii) The components of $\boldsymbol{D}^{n+1}$ are computed from $\boldsymbol{H}$.
(iv) The components of $\boldsymbol{E}^{n+1}$ are obtained from $\boldsymbol{D}$.
(v) Return to (i).

Because the invalidity of the differential forms of the Maxwell equations at the material boundary, the parameter mean method is used. The results below prove the validity of the parameter mean method, otherwise, the program will be divergent.

4. NUMERICAL RESULTS AND DISCUSSIONS

Continuous wave (CW) Gaussian beam propagation in multi-layered structures that include four classes of AMM is investigated with shift operator method in FDTD in this section.

The 2D-FDTD simulator solves the equivalent TE wave set for E_y, H_x, and H_z. The cell sizes are $\Delta x = \Delta z = 0.02\,\text{cm}$ long, corresponding to $\lambda_0/50$. The time step is set to be $\Delta t = \Delta z/2c$. The CW Gaussian beam $s(t) = \sin(\omega_0 t)$ is launched into the total field region using a total-scattered field (TF-SF) formulation. t is the observation time. The CW frequency is chosen to be $f_0 = 30\,\text{GHz}$. The focal plane of the beam is taken to be the TF-SF boundary. The beam varies spatially as $\exp(-x^2/w_0^2)$ on that boundary, i.e., its amplitude falls to e^{-1} at its waist $w_0 = 50\Delta z$. The boundaries of different media are outlined with solid lines. Except for Always Cutoff media slabs case, $\varepsilon_1 = 12.8$ and $\mu_1 = \varepsilon_2 = \mu_2 = 1$ are chosen for the following parameters of medium 1 and medium 2 in multi-layered structures. By properly choosing the ε_y, μ_x and μ_z in the relative permittivity and permeability tensors, various anisotropic material parameters of AMM slabs can be obtained.

4.1. Cutoff Media Slabs Case

Figure 2 gives electric field intensity distributions for the interaction of the Gaussian beam with multi-layered structures that include one subtype of Cutoff media and dispersion plot for Cutoff media. The validity of method and program can be seen in reference [23].

Reference [11] only gave the excitation of guided waves in layered structures that include isotropic metamaterials. The materials parameters selected in Figs. 2(a) and (b) make Cutoff media much more like an isotropic medium. In Fig. 2(a), the maximum of surface wave shifted in the direction opposite to the direction of the incident wave indicated that the excited wave at the boundary between air and

Cutoff media is backward. Because the materials parameters selected in Fig. 2(b) are not satisfied with the conditions $|\varepsilon_3\mu_3|/(\varepsilon_2\mu_2) > 1$ and $|\mu_3|/\mu_2 < 1$, the process of the excitation of the forward surface wave can be clearly observed. The interface between medium one and two generates reflected and transmitted beams. These two kinds of beams interact with each other. The surface wave can transfer the energy along the interface between medium two and three leading to an effective enhancement of the lateral shift of the reflected and transmitted beams.

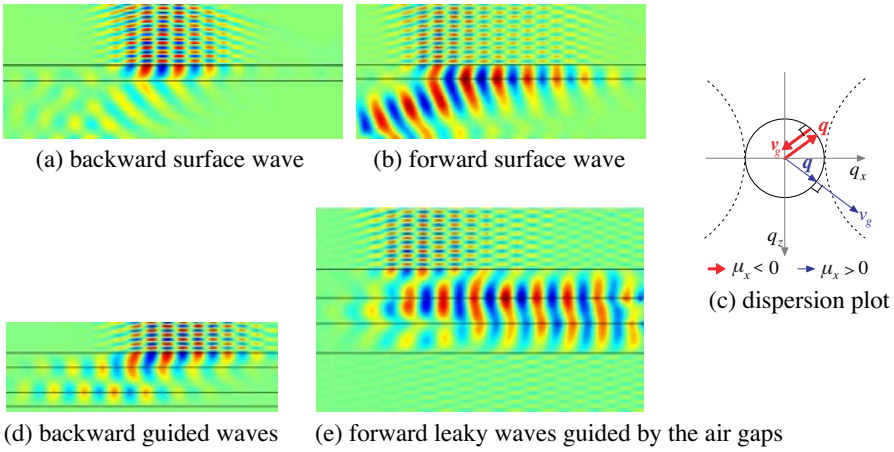

Figure 2. FDTD predicts field intensity distributions for Gaussian beam propagation in multi-layered structures include Cutoff media subtype I having (a) $\varepsilon_3 = -3$, $\mu_3 = -0.5$, $d = 0.5\lambda_0$, $t = 3500\Delta t$, $\theta = 74°$, (b) $\varepsilon_3 = -0.5$, $\mu_3 = -2$, $d = 0.5\lambda_0$, $t = 5000\Delta t$, $\theta = 74°$, (c) dispersion plot, (d) $\varepsilon_y = -3$, $\mu_x = -0.6$, $\mu_z = -0.4$, $d = 0.5\lambda_0$, $L = 0.8\lambda_0$, $t = 3700\Delta t$, $\theta = 69°$, and (e) $\varepsilon_y = -0.5$, $\mu_x = -2.2$, $\mu_z = -1.8$, $d = \lambda_0$, $L = 0.8\lambda_0$, $t = 6700\Delta t$, $\theta = 71°$.

In Fig. 2(c), $\boldsymbol{q}$ and $\boldsymbol{v}_q$ specifies the directions of wave vector and energy flow density $\boldsymbol{S}$ in Cutoff media slabs. The directions of $\boldsymbol{q}$ and $\boldsymbol{v}_g$ are antiparallel in subtype I of Cutoff media, however they are parallel in subtype II of Cutoff media. According to the energy flow density $\boldsymbol{S}$ in AMM

$$S = \mathrm{Re}\left[\frac{T_{\mathrm{TE}}^2 E_0^2 q_x}{2\omega\mu_0\mu_z}\hat{x} + \frac{T_{\mathrm{TE}}^2 E_0^2 q_z}{2\omega\mu_0\mu_x}\hat{z}\right] \tag{10}$$

the dispersive curve is circle if the Cutoff media is isotropic ($\mu_x = \mu_z$) and elliptic if the Cutoff media is anisotropic ($\mu_x \neq \mu_z$).

The Cutoff media in Figs. 2(d) and (e) is not an isotropic medium. The excited backward guided wave in Fig. 2(d) has a vortex-like shape. The lateral direction of wave vector and energy flow in Cutoff media is opposite to those in common media or air. Fig. 2(e) shows that the waves excited by the leaky waves are guided by the air gap.

4.2. Never Cutoff Media Slabs Case

Figure 3 presents electric field intensity distributions for wave propagation in three-layered structures that include two subtypes of Never Cutoff media and dispersion plot for Never Cutoff media. Comparing Figs. 3(a) and (b), one finds that electric field is mostly concentrated in the air gaps. However, the wave vector and energy flow density of the leaky wave in two subtypes of Never Cutoff media are no longer parallel or antiparallel just as those depicted in Fig. 3(d). As shown in Fig. 3(a), wave vector is backward and anomalous refractions occur in subtype I of Never Cutoff media, whereas the energy flow is positively refracted in subtype I of Never Cutoff media slab. Though the wave vector is forward in Fig. 3(c), i.e., regular refractions occur in subtype II of Never Cutoff media, the shift of Gaussian beam

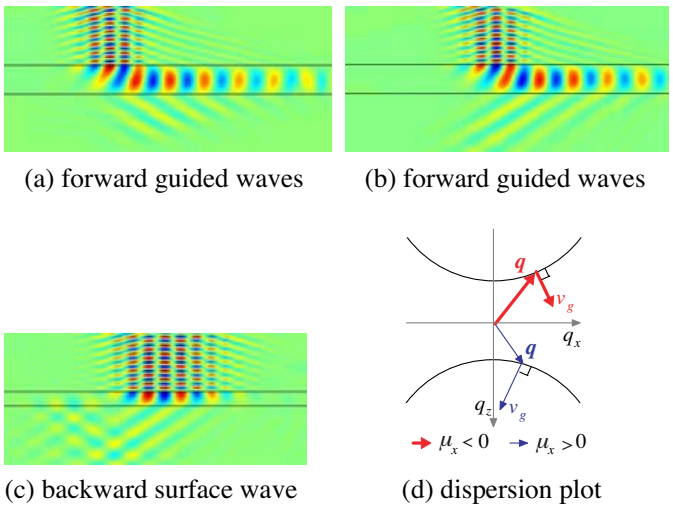

Figure 3. FDTD predicts field intensity distributions for Gaussian beam incident at $\theta = 70°$ to three-layered structures that include Never Cutoff media subtype I having $\varepsilon_y = -2$, $\mu_x = -0.5$, $\mu_z = 0.5$, (a) $d = \lambda_0$, $t = 1900\Delta t$, and subtype II having ε_y=2, $\mu_x = 0.5$, $\mu_z = -0.5$, (b) $d = \lambda_0$, $t = 2000\Delta t$, (c) $d = 0.5\lambda_0$, $t = 3600\Delta t$, (d) dispersion plot.

propagating in the AMM slab is negative and the backward surface wave is excited at the boundary between air and subtype II of Never Cutoff media. It can be explained as whether the wave vector refraction is regular or anomalous are determined by the sign of μ_x, and whether the energy flow is positively or negatively refracted are determined by the sign of μ_z [10]. The backward surface wave can be excited even if the constants in the relative permittivity and permeability tensors of anisotropic metamaterial are not all negative. As theoretical investigation in reference [15], a compact and very efficient beam splitter based on large birefringence can be only made of AMM slab to route wave, if one polarized wave is positively refracted ($v_{gx} > 0$) whereas the other is negatively refracted ($v_{gx} < 0$). The AMM slab can be realized with ring and rod.

4.3. Anti-Cutoff Media Slabs Case

Figure 4 shows the Gaussian beam propagation in five-layered structures that include two subtypes of Anti-Cutoff media and dispersion plot for Anti-Cutoff media. Backward guided waves are excited at the boundary between air and subtype II of Anti-Cutoff media. The conditions for the excitation of the backward surface waves if the third medium is anisotropic medium are not restricted by those if the third medium is isotropic metamaterial. Because $\mu_z < 0$, the energy flow density is negatively refracted, even if the wave vector is forward. The amplitude of the backward guided wave is lower than the incident wave. The forward guided waves can be treated as excitations of leaky waves that are guided by the air gaps.

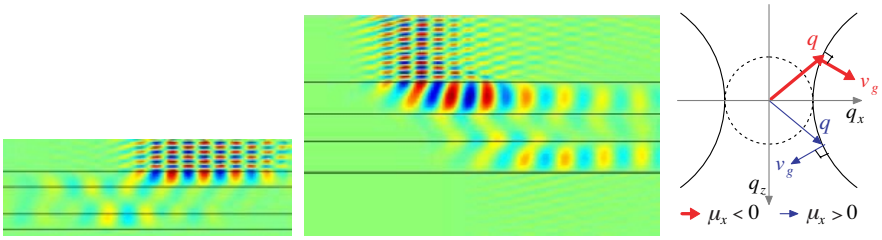

(a) backward guided waves (b) forward leaky waves (c) dispersion plot

Figure 4. FDTD predicts field intensity distributions for Gaussian beam propagation in five-layered structures that include Anti-Cutoff media (a) subtype II having $\varepsilon_y = -2$, μ_x=0.2, $\mu_z = -0.2$, $d = 0.5\lambda_0$, $L = 0.8\lambda_0$, $t = 4000\Delta t$, $\theta = 75°$, and (b) subtype I having $\varepsilon_y = 2$, $\mu_x = -0.2$, $\mu_z = 0.2$, $d = \lambda_0$, $L = 0.8\lambda_0$, $t = 2800\Delta t$, $\theta = 70°$, (c) dispersion plot.

4.4. Always Cutoff Media Slabs Case

Due to total reflection always occurs when the beam incident from isotropic medium to Always Cutoff media slabs at any angle. Fig. 5 presents FDTD predicting the electric intensity distributions for the interaction between Gaussian beam and two types of Always Cutoff media slabs. Positive or negative Goos-Hänchen shift phenomena occur. To every kind of EM field, the sign of Goos-Hänchen shift for the two types of Always Cutoff AMM are opposite. However for Never Cutoff media, total reflection phenomena never occurs at any incident angle. Omnidirectional linear polarizer can be realized by AMM slab, if one polarized wave is omnidirectional total transmission whereas the other is omnidirectional total reflection.

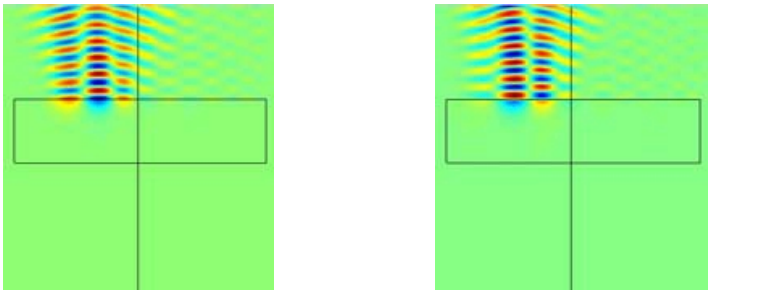

(a) subtype I, ε_y= -0.5, μ_x=0.5, μ_z=1 (b) subtype II, ε_y =0.5, μ_x=-0.5, μ_z =-1

Figure 5. FDTD predicts electric field intensity distributions for the Gaussian beam that is incident at 30° from isotropic media with $\mu_1 = \varepsilon_1 = 2$, $\varepsilon_3 = \mu_3 = 1$ to an Always Cutoff AMM slabs, $d = 2\lambda_0$, $t = 7500\Delta t$.

According to the principle of duality, the interaction of TM-polarized Gaussian beam and multi-layered structures that include AMM can also be simulated (not shown in the paper).

5. CONCLUSIONS

We have derived the shift operator method in FDTD. The Gaussian beam propagation in multi-layered structures that include indefinite AMM is investigated with shift operator in FDTD. From the numerical results shown in the paper, one can find that for TE-polarized wave, the sign of z component of relative permeability tensor of AMMs determines the energy flow is positively refracted or negatively refracted in AMMs. Thus the backward surface wave at the material

boundary can be excited if $\mu_z < 0$ and the forward surface wave can be excited if $\mu_z > 0$. The direction of the guided waves affected by the sign of μ_x is small. Some potential applications in solid-state spectroscopy, beam splitter and linear polarizer for AMMs are discussed. Nonetheless, their eventual usefulness for the potential practical applications will depend greatly on clever fabrication concepts and implementations in those scenarios.

ACKNOWLEDGMENT

This work was supported by National Key Laboratory of Electromagnetic Environment fund under Grant No. 51486030305HT0101 and 9140C08060507ZCZJ18.

REFERENCES

1. Veselago, V. G., "The electrodynamics of substances with simultaneously negative values of ε and μ," *Sov. Phys. Usp.*, Vol. 10, No. 4, 509–514, 1968.
2. Pendry, J. B., A. J. Holden, D. J. Robbins, and W. J. Stewart, "Magnetism from conductors and enhanced nonlinear phenomena," *IEEE Trans. Microwave Theory Tech.*, Vol. 47, No. 11, 2075–2084, 1999.
3. Shelby, R. A., D. R. Smith, and S. Schultz, "Experimental verification of a negative index of refraction," *Science*, Vol. 292, No. 6, 77–79, 2001.
4. Chen, H., B.-I. Wu, and J. A. Kong, "Review of electromagnetic theory in left-handed materials," *Journal of Electromagnetic Waves and Applications*, Vol. 20, No. 15, 2137–2151, 2006.
5. Grzegorczyk, T. M. and J. A. Kong, "Review of left-handed metamaterials: Evolution from theoretical and numerical studies to potential applications," *Journal of Electromagnetic Waves and Applications*, Vol. 20, No. 14, 2053–2064, 2006.
6. Eleftheriades, G. V., "Enabling RF/Microwave devices using negative-refractive-index transmission-line (NRI-TL) metamaterials," *IEEE Antennas and Propagation Magazine*, Vol. 49, No. 2, 34–51, 2007.
7. Grzegorczyk, T. M., C. D. Moss, J. Lu, X. Chen, J. Jr. Pacheco, and J. A. Kong, "Properties of left-handed metamaterials: Transmission, backward phase, negative refraction, and focusing," *IEEE Trans. Microwave Theory Tech.*, Vol. 53, No. 9, 2956–2967, 2005.

8. Yao, H. Y., W. Xu, L. W. Li, Q. Wu, and T.-S. Yeo, "Propagation property analysis of metamaterial constructed by conductive SRRs and wires using the MGS-based algorithm," *IEEE Trans. Microwave Theory Tech. (Special Issue on Metamaterials)*, Vol. 53, No. 4, 1469–1476, 2005.
9. Lindell, I. V., S. A. Tretyakov, K. I. Nikoskinen, and S. Ilvonen, "BW media-media with negative parameters, capable of supporting backward waves," *Microwave and Optical Technology Letters*, Vol. 31, No. 2, 129–133, 2001.
10. Smith, D. R. and D. Schurig, "Electromagnetic wave propagation in media with indefinite permittivity and permeability tensors," *Physical Review Letters*, Vol. 90, No. 7, 077405, 1–4, 2003.
11. Shadrivov, I. V., R. W. Ziolkowski, A. A. Zharov, and Y. S. Kivshar, "Excitation of guided waves in layered structures with negative refraction," *Optics Express*, Vol. 13, No. 2, 481–492, 2005.
12. Grzegorczyk, T. M., X. Chen, Jr. J. Pacheco, J. Chen, B. I. Wu, and J. A. Kong, "Reflection coefficients and Goos-Hänchen shifts in anisotropic and bianisotropic left-handed metamaterials," *Progress In Electromagnetics Research*, PIER 51, 83–113, 2005.
13. Xiang, Y. J., X. Y. Dai, and S. C. Wen, "Total reflection of electromagnetic waves propagating from an isotropic medium to an indefinite metamaterial," *Optics Communications*, Vol. 274, No. 1, 248–253, 2007.
14. Shen, N., Q. Wang, J. Chen, et al., "Total transmission of electromagnetic waves at interfaces associated with an indefinite medium," *Journal of the Optical Society of America B*, Vol. 23, No. 5, 904–912, 2006.
15. Luo, H., Z. Ren, W. Shu, and F. Li, "Construct a polarizing beam splitter by an anisotropic metamaterial slab," *Appl. Phys. B*, Vol. 87, 283–287, 2007.
16. Thomas, Z. M., T. M. Grzegorczyk, B. I. Wu, et al., "Design and measurement of a four-port device using metamaterials," *Optics Express*, Vol. 13, No. 12, 4737–4744, 2005.
17. Semouchkina, E. A., G. B. Semouchkin, M. Lanagan, and C. A. Randall, "FDTD study of resonance processes in metamaterials," *IEEE Trans. Microwave Theory Tech.*, Vol. 53, No. 4, 1477–1487, 2005.
18. Nader, E. and R. W. Ziolkowski, "A positive future for Double-Negative metamaterials," *IEEE Trans. Microwave Theory Tech.*, Vol. 53, No. 4, 1535–1556, 2005.

19. Ziolkowski, R. W. and E. Heyman, "Wave propagation in media having negative permittivity and permeability," *Physics Review E*, Vol. 64, No. 5, 056625, 1–15, 2001.
20. Wang, M. Y., J. Xu, J. Wu, Y. B. Yan, and H. L. Li, "FDTD study on scattering of metallic column covered by double-negative metamaterial," *Journal of Electromagnetic Waves and Applications*, Vol. 21, No. 14, 1905–1914, 2007.
21. Grande, A., J. A. Pereda, O. González, et al., "FDTD modeling of double negative metamaterials characterized by high-order frequency-dispersive constitutive parameters," *Antennas and Propagation Society International Symposium 2006*, IEEE, 4603–4606, 2007.
22. Shi, Y. and C.-H. Liang, "Analysis of the double-negative materials using multi-domain pseudospectral time-domain algorithm," *Progress In Electromagnetics Research*, PIER 51, 153–165, 2005.
23. Wang, M. Y., D. B. Ge, J. Xu, and J. Wu, "FDTD study on back scattering of conducting sphere coated with double-negative metamaterials," *International Journal of Infrared and Millimeter Waves*, Vol. 28, No. 2, 199–206, 2007.
24. Zainud-Deen, S. H., A. Z. Botros, and M. S. Ibrahim, "Scattering from bodies coated with metamaterial using FDTD method," *Progress In Electromagnetics Research B*, Vol. 2, 279–290, 2008.
25. Ding, W., L. Chen, and C. H. Liang, "Numerical study of Goos-Hänchen shift on the surface of anisotropic left-handed materials," *Progress In Electromagnetics Research B*, Vol. 2, 151–164, 2008.